Math. Res. Lett.
Volume 25, Number 5, 1497–1524, 2018

Trisections and spun four-manifolds

Jeffrey Meier

We study trisections of 4–manifolds obtained by spinning and twist-spinning 3–manifolds, and we show that, given a (suitable) Heegaard diagram for the 3–manifold, one can perform simple local modifications to obtain a trisection diagram for the 4–manifold. We also show that this local modification can be used to convert a (suitable) doubly-pointed Heegaard diagram for a 3–manifold/knot pair into a doubly-pointed trisection diagram for the 4–manifold/2–knot pair resulting from the twist-spinning operation.

This technique offers a rich list of new manifolds that admit trisection diagrams that are amenable to study. We formulate a conjecture about 4–manifolds with trisection genus three and provide some supporting evidence.

1. Outline

The theory of trisections was introduced by Gay and Kirby as a novel way of studying the smooth topology of 4–manifolds [13]. Since then, the theory has developed in a number of directions: Extensions of the theory to the settings of manifolds with boundary [8–11], knotted surfaces [29, 30], algebraic objects [1, 25], and higher dimensional manifolds [37] have been established; programs offering connections with singularity theory [4, 5, 12–15], and Dehn surgery [27, 31], have been initiated; some classification results have been obtained [27, 28]; interpretations of constructions and cut-and-paste operation have been explored [16, 26]; and new invariants have been proposed [19, 23, 38]. The purpose of this note is two-fold: motivate an extension of the classification program and generate a rich set of examples of manifolds with trisection diagrams that are simple enough to be amenable to study.

Manifolds with trisection genus at most one are easy to classify [13]. In [28], it was shown that $S^2 \times S^2$ is the unique irreducible[1] manifold with

[1]We call a 4–manifold X *irreducible* if each summand of any connected sum decomposition of X is either X or a homotopy 4–sphere.

trisection genus two, and it was asked to what extent it is possible to enumerate manifolds with trisection genus g for low values of g. To this end, we offer the following conjecture.

Conjecture 1.1. *Every irreducible 4–manifold with trisection genus three is either the spin of a lens space, or a Gluck twist on a specific 2–knot in the spin of a lens space.*

These manifolds have rich but fairly obfuscated history of study in the literature, which we aim to unify in the discussion below. Since there is a unique spun lens space for each $p \in \mathbb{N}$ and at most one additional manifold obtained by the specified Gluck twist, this conjecture would give an extremely simple enumeration of manifolds admitting minimal genus $(3,1)$–trisections.

(Note that $(3,2)$–trisections are trivial in a precise sense [27], while $(3,0)$–trisections are conjecturally trivial in the same sense, so Conjecture 1.1 can really the thought of as a conjecture about manifolds with irreducible $(3,1)$–trisections.) At the end of the paper, we present diagrams for the subjects of Conjecture 1.1.

Given a closed, connected, orientable 3–manifold M, let $\mathcal{S}(M)$ and $\mathcal{S}^*(M)$ denote the *spin* and *twisted-spin* of M, respectively. (See Section 3 for precise definitions.)

Theorem 1.2. *Suppose that M admits a genus k Heegaard splitting. Then $\mathcal{S}(M)$ and $\mathcal{S}^*(M)$ admit $(3k,k)$–trisections.*

An immediate application of this theorem is an explicit description of 4–manifolds admitting minimal genus trisections of arbitrarily large genus.

Corollary 1.3. *For every integer $g \geq 3$ and every $1 \leq k \leq g-2$, there exist infinitely many distinct 4–manifolds admitting minimal (g,k)–trisections.*

A similar corollary has been independently obtained recently by Baykur and Saeki [5]. Corollary 1.3 becomes more interesting in light of our ability to give diagrams for the pertinent trisections.

Theorem 1.4. *Let (S,δ,ε) be a genus g Heegaard diagram for a closed 3–manifold M with the property that H_ε is standardly embedded in S^3. Then the 4–manifolds $\mathcal{S}(M)$ and $\mathcal{S}^*(M)$ each admit a trisection diagram that is obtained from (S,δ,ε) via a local modification at each curve of ε.*

The local moves are described in Figures 6 and 7. See Section 3 for a more detailed statement of the above theorem.

Finally, we consider what happens when the twist-spinning construction is applied to a 3–manifold/knot pair. Our main result to this end is that the twisted-spin of a doubly-pointed Heegaard diagram is a doubly-pointed trisection diagram. This latter object describes not only the trisected 4–manifold, but also a knotted sphere therein. Given a 3-manifold/knot pair (M, K), let $\mathcal{S}^n(M, K)$ denote the n–twist-spin of (M, K).

Theorem 1.5. *Let (S, δ, ε) be a genus g Heegaard diagram for a closed 3–manifold M with the property that H_ε is standardly embedded in S^3. Let K be a knot in M such that $(S, \delta, \varepsilon, z, w)$ is a doubly-pointed Heegaard diagram for the pair (M, K). Then the pairs $\mathcal{S}^n(M, K)$ admit doubly-pointed trisection diagrams that are obtained from $(S, \delta, \varepsilon, z, w)$ via a local modification at each curve of ε.*

Organization

Section 2 presents general background material regarding spinning and twist-spinning, Heegaard splittings and trisections, and doubly-pointed diagrams. In Section 3, we give a singularity theoretic proof of Theorem 1.2, and more geometric proofs of Theorems 1.4 and 1.5, the former of which also recovers a proof of Theorem 1.2. In Section 4, we prove Corollary 1.3, discuss Conjecture 1.1, give a number of examples, and pose some questions.

2. Background

2.1. Spun 4–manifolds and 2–knots

We recall the set-up of spun 4–manifolds, as well as some classical results about these spaces. Given a closed, connected 3–manifold M, we let $\mathcal{S}(M)$ and $\mathcal{S}^*(M)$ denote the *spin* and *twisted-spin* of M, respectively. These manifolds are given as follows:

$$\mathcal{S}(M) = (M^\circ \times S^1) \cup_{\mathrm{id}} (S^2 \times D^2),$$

and

$$\mathcal{S}^*(M) = (M^\circ \times S^1) \cup_{\tau} (S^2 \times D^2),$$

where τ is the unique self-diffeomorphism of $S^2 \times S^1$ not extending over $S^2 \times D^2$ [17]. Adopting coordinates (h, ϕ) for S^2, where $h \in [-1, 1]$ represents

distance from the equator and $\phi \in S^1$ is angular displacement from a fixed longitude, this map is given by

$$\tau((h, \phi), \theta) = ((h, \phi + \theta), \theta).$$

In other words, τ twists S^2 through one full rotation as we traverse the S^1 direction. In fact, one could consider gluings using powers of τ, but the resulting manifold will only depend (up to diffeomorphism) on the parity of the power [17].

Such spaces were well studied in the 1980s and earlier. Here, we will summarize some of the more pertinent facts. We denote diffeomorphism and homotopy-equivalence by $\cong$ and $\simeq$, respectively. It appears that a complete classification of when the spin and twisted-spin of a given 3–manifold are diffeomorphic remains open. However, we have the following significant progress due to Plotnick.

Theorem 2.1 (Plotnick [35]). *Let M be a closed, connected, orientable 3–manifold.*

1) *If M is aspherical, then $\mathcal{S}(M) \ncong \mathcal{S}^*(M)$.*
2) *$\mathcal{S}(M) \cong \mathcal{S}^*(M)$ if every summand of M is either $S^1 \times S^2$ or a spherical 3–manifold with all Sylow subgroups of $\pi_1(M)$ cyclic.*

Remark 2.2. Note that $\mathcal{S}(M)$ and $\mathcal{S}^*(M)$ have identical 3–skeleta. One way to see this is to notice that both of these manifolds are obtained from $M \times S^1$ by surgering a circle $* \times S^1$, with the result only depending on the choice of framing in $\pi_1(SO(3)) \cong \mathbb{Z}_2$. Since the framings can be assumed to agree on a portion of $* \times S^1$, it follows that the surgeries differ only in the attaching of a 4–cell. As a consequence $\pi_1(\mathcal{S}(M)) \cong \pi_1(\mathcal{S}^*(M))$, and it is not hard to argue that this group is simply $\pi_1(M)$.

By the above remark, $\mathcal{S}(L(p, q))$ can be obtained by surgering out $S^1 \times *$ inside $S^1 \times L(p, q)$. Pao observed that $\mathcal{S}(L(p, q))$ can also be obtained by surgering the simple closed curve in $S^1 \times S^3$ representing $p \in \mathbb{Z} \cong \pi_1(S^1 \times S^3)$ [34]. As in Remark 2.2, there are two choices for the framing of such a surgery. Let $\mathcal{S}_p$ and $\mathcal{S}'_p$ denote the manifolds obtained from surgery on the winding number p curve in $S^1 \times S^3$. (Note that it follows that $\mathcal{S}_p$ and $\mathcal{S}'_p$ are related by a Gluck twist on the belt-sphere of this surgery.) Pao proved the following.

Proposition 2.3 (Pao [34]).

1) $\mathcal{S}_p \cong \mathcal{S}(L(p,q))$.

2) $\mathcal{S}'_p \cong \mathcal{S}_p$ *if* p *is odd and* $\mathcal{S}'_p \ncong \mathcal{S}_p$ *if* p *is even.*

We remark that it is not clear whether Pao identified $\mathcal{S}_p$ as a spun lens space, though it appears that Plotnick made the connection [35]. (See also [40].) Moreover, many authors who have studied Pao's manifolds since seem not to have noted the connection with spun lens spaces, instead studying them as manifolds admitting genus one broken Lefschetz fibrations [3, 5, 21].

Combining Theorem 2.1(2) and Proposition 2.3(1), we have the following corollary.

Corollary 2.4. *For all* $1 \leq q < p$, *both* $\mathcal{S}(L(p,q))$ *and* $\mathcal{S}^*(L(p,q))$ *are diffeomorphic to* $\mathcal{S}_p$.

We will let $\mathcal{P} = \{\mathcal{S}_p\}_{p\in\mathbb{N}} \cup \{\mathcal{S}'_p\}_{p\in 2\mathbb{N}}$ be the set of Pao's manifolds, and we will refer to the $\mathcal{S}_p$ as the *spun lens spaces* and to the $\mathcal{S}'_p$ as their *siblings*.

Remark 2.5. Note that there are two pertinent 2–knots in the manifold $\mathcal{S}_p = \mathcal{S}(L(p,q))$. The first is the core of the $D^2 \times S^2$ used in the spinning construction. Performing a Gluck twist on this 2–knot results in $\mathcal{S}^*(L(p,q))$, while surgery yields $S^1 \times L(p,q)$. The second 2–knot has the property that surgery yields $S^1 \times S^3$; thus, it cannot be isotopic to the first 2–knot. Performing a Gluck twist on this latter 2–knot results in the sibling manifold $\mathcal{S}'_p$.

Finally, we extend the definition of twist-spinning to 3–manifold/knot pairs. For a fixed 3–manifold M and a knot K in M, let $\mathcal{S}^n(M,K)$ denote the *n–twist-spin* of the pair (M,K):

$$\mathcal{S}^n(M,K) = ((M,K)^\circ \times S^1) \bigcup_{\tau^n} (S^2 \times D^2, \{\mathfrak{n},\mathfrak{s}\} \times D^2),$$

where the gluing is via the n–fold power of the Gluck twist map defined above. We write $\mathcal{S}^k(M,K) = (\mathcal{S}^k(M), \mathcal{S}^k(K))$. Since τ^2 extends over $S^2 \times D^2$, we have that $\mathcal{S}^k(M)$ is either $\mathcal{S}(M)$ or $\mathcal{S}^*(M)$ (based on whether k is even or odd). On the other hand, the 2–knots $\mathcal{S}^k(K)$ will likely represent different isotopy classes as k varies.

When $M \cong S^3$, the resulting twist-spun knots $\mathcal{S}^n(K)$ have been well studied, starting with Zeeman [41], who introduced the general notion (following Artin [2]). On the other hand, it appears that very little attention has been focused on the case of twist-spinning knots in non-trivial 3–manifolds.

2.2. Heegaard splittings and trisections

We briefly recall the basic set-up of the theories of Heegaard splittings and trisections. A *genus g Heegaard splitting* of a closed, connected, orientable 3–manifold M is a decomposition

$$M = H_\delta \cup_\Sigma H_\varepsilon,$$

where H_δ and H_ε are handlebodies whose common boundary is a closed surface Σ of genus g. Every closed 3–manifold admits a Heegaard splitting [6, 32], and any two Heegaard splittings of a fixed manifold are stably equivalent [36, 39].

Let δ be a collection of g disjoint curves on Σ arising as the boundary of g properly embedded disks in H_δ and satisfying the property that $\Sigma \setminus \nu(\delta)$ is connected and planar. Let ε be a similar collection of curves corresponding to H_ε. The triple $(\Sigma, \delta, \varepsilon)$ is called a *Heegaard diagram* for the splitting $M = H_\delta \cup_\Sigma H_\varepsilon$. Any two diagrams for a given splitting can be related by handleslides (among the respective sets of curves) and diffeomorphism [24].

A (g,k)*–trisection* of a smooth, orientable, connected, closed 4–manifold X is a decomposition $X = X_1 \cup X_2 \cup X_3$, where

1) each X_i is a 4–dimensional 1–handlebody, $\natural^k(S^1 \times B^3)$;
2) for $i \neq j$, each of $X_i \cap X_j$ is a three-dimensional handlebody, $\natural^g(S^1 \times D^2)$; and
3) the common intersection $\Sigma = X_1 \cap X_2 \cap X_3$ is a closed surface of genus g.

The surface Σ is called the *trisection surface*, and the *genus* of the trisection is said to be $g = g(\Sigma)$. The *trisection genus* of a 4–manifold X is the smallest value of g for which X admits a trisection of genus g, but no trisection of smaller genus.

Note that Σ is a Heegaard surface for $\partial X_i \cong \#^k(S^1 \times S^2)$, so $0 \leq k \leq g$. As in the case of Heegaard splittings, every smooth 4–manifold admits a trisection, and any two trisections for a fixed 4–manifold are stably equivalent [13].

A *trisection diagram* is a quadruple $(\Sigma, \alpha, \beta, \gamma)$ where each triple (Σ, α, β), etc., is a Heegaard diagram for $\#^k(S^1 \times S^2)$. As before, any two diagrams corresponding to a given splitting can be made diffeomorphic after handleslides within each collection of curves. See [13, 27] for complete details.

2.3. Doubly-pointed diagrams

A *doubly-pointed* Heegaard diagram is a tuple $(\Sigma, \delta, \varepsilon, z, w)$, consisting of a Heegaard diagram, together with a pair of base points, z and w, in $\Sigma \setminus \nu(\delta \cup \varepsilon)$. Suppose the underlying Heegaard diagram describes the 3–manifold M. Then, the base points encode a knot K in M in the following way. Let υ_δ and υ_ε be arcs connecting z and w in $\Sigma \setminus \nu(\delta)$ and $\Sigma \setminus \nu(\varepsilon)$, respectively. Equivalently, υ_δ and υ_ε are boundary parallel arcs contained in the 0–cells of the respective handlebodies. The knot K is the the union of these two (pushed-in) arcs along their common end points, z and w. The following theorem is standard.

Theorem 2.6. *Given any 3–manifold/knot pair (M, K), there is a doubly-pointed Heegaard diagram describing (M, K).*

A *doubly-pointed* trisection diagram is a tuple $(\Sigma, \alpha, \beta, \gamma, z, w)$ where each sub-tuple $(\Sigma, \alpha, \beta, z, w)$, etc., is a doubly-pointed Heegaard diagram for $(\#^k(S^1 \times S^2), U)$, where U is the unknot. Suppose the underlying trisection diagram describes the 4–manifold X. Then the base points encode a knotted sphere $\mathcal{K}$ in X in the following way. Let $D_i \subset \partial X_i$ be spanning disks for the three unknots described by the diagram. Let $\mathcal{K}$ be the union of these three disks, after the interiors of the disk have been isotoped to lie in the interiors of the X_i.

The decomposition $(X, \mathcal{K}) = (X_1, D_1) \cup (X_2, D_2) \cup (X_3, D_3)$ is called a *1–bridge trisection* of the pair $(X, \mathcal{K})$, and $\mathcal{K}$ is said to be in *1–bridge position* with respect to the underlying trisection of X. The following results are proved in [30].

Theorem 2.7. *Let X be a smooth, orientable, connected, closed 4–manifold, and let $\mathcal{K}$ be a knotted sphere in X. There exists a trisection of X with respect to which $\mathcal{K}$ can be isotoped to lie in 1–bridge position.*

Corollary 2.8. *For any 4–manifold/2–knot pair $(X, \mathcal{K})$, there is a doubly-pointed trisection diagram describing $(X, \mathcal{K})$.*

3. Proof of main theorems

In this section, we give the proofs for the main theorems described in the introduction. First, we will adopt the Morse 2–function perspective to prove that both the spin and twisted-spin of a 3–manifold admitting a genus g Heegaard splitting admit $(3g, g)$–trisections.

Roughly, for a smooth, orientable, connected, closed 4–manifold X, a map $F\colon X \to \mathbb{R}^2$ is a *Morse 2–function* if

1) Every regular value $y \in \mathbb{R}^2$ has a neighborhood D^2 such that F is projection $S \times D^2 \to D^2$ for some closed surface S.
2) The set of critical points of F is a smooth one-dimensional submanifold whose image in $\mathbb{R}^2$ is a collection of immersed curves with isolated crossings and semi-cubical cusps.
3) Every critical value $y \in \mathbb{R}^2$ has local coordinates such that F looks like a generic homotopy of a Morse function: If y is a cusp, F looks like the birth of a canceling pair of Morse critical points. If y is a crossing point, F looks like two Morse critical points swapping height. If y is not on a cusp or a crossing point, F looks like a Morse critical point times I.

See [13] for a complete definition. See also [5] for a detailed overview of various types of generic functions from 4–manifolds to surfaces.

We now sketch a quick, Morse 2–function proof of our first result, which was first conceived by Alex Zupan. Our proof of Theorem 1.4, below, will provide a second, independent proof of this result.

Theorem 1.2. Suppose that M admits a genus g Heegaard splitting. Then each of $\mathcal{S}(M)$ and $\mathcal{S}^*(M)$ admits a $(3g, g)$–trisection.

Proof. Let M be a closed, connected, orientable 3–manifold, and suppose that M admits a genus g Heegaard splitting $\mathcal{H}$. Let $f\colon M \to \mathbb{R}$ be a Morse function corresponding to $\mathcal{H}$, and suppose that f has isolated critical points of non-decreasing index.

Consider the 4–manifold $\bar{X} = M \times S^1$, and let $\bar{F}\colon X \to \mathbb{R}^2$ be the Morse 2–function induced fiber-wise by the Morse function f. See Figure 1(a). The map $\bar{F}$ has a single (definite) fold of both indices zero and three, as well as g indefinite folds of both indices one and two. Note that $\bar{F}(\bar{X})$ is an annulus. We decorate indefinite folds with arrows that point from the higher genus side of the fold to the lower genus side.

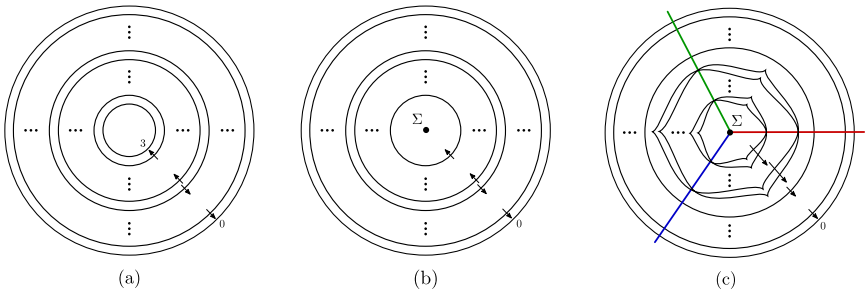

Figure 1: (a) The Morse 2–function $\bar{F}$ on $\bar{X} = M \times S^1$ induced by a Morse function f on M with isolated critical points of non-decreasing index. (b) The corresponding Morse 2–function F on the manifold X obtained as surgery on the round three-handle inside $\bar{X}$. (c) The trisected Morse 2–function homotopic to F with no folds of index two.

Finally, let X denote a 4–manifold obtained from $\bar{X}$ by surgering out the round three-handle, whose core projects to the fold of index three. In other words, cut out the $B^3 \times S^1$ corresponding the the $h_3 \times S^1$, where h_3 is the three-handle of M, and glue in a copy of $S^2 \times D^2$. In fact, there are two ways to do this [17]. One choice results in $\mathcal{S}(M)$, the other in $\mathcal{S}^*(M)$. However, this distinction is not visible in the base diagrams of the Morse 2–functions, so we will simply let X denote either choice.

Let $F\colon X \to \mathbb{R}^2$ denote the resulting Morse 2–function, which differs from $\bar{F}$ in that it has no (definite) fold of index three, and $F(X)$ is a disk. See Figure 1(b). Note that the fiber Σ over the central point of the disk is a two-sphere. To complete the proof, we will homotope F, using standard moves, until it has no folds of index two or greater. To do this, we will take each fold of index two and transform it into an immersed fold of index one containing six cusps. We can do this one index two fold at a time, and we illustrate this sub-process in Figure 2.

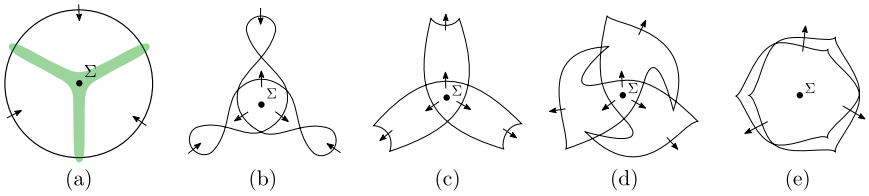

Figure 2: The process (from left to right) of turning a index two fold inside out. Arrows indicate the direction of decrease of the fiber genus.

First, we select three points on the index two fold and drag them radially towards and past the center point, this can be seen as a sort of a contraction of the shaded area in Figure 2(a), which results in Figure 2(b). This is accomplished via a $R2_0$ move followed by a $R3_3$ move. (See [5] for details. All base diagram moves employed here are always-realizable.) Next, we turn each of the three kinks into a pair of cusps, resulting in Figure 2(c). This can be accomplished via three instances of the flip move, each followed by a $R2_2$ move. Note that the genus of Σ has been increased by three. Figure 2(d) follows via three C-moves, and Figure 2(e) follows after three $R2_2$ moves.

After the above process has been carried out on the innermost indefinite fold of index two in Figure 1(b), the resulting six-cusped fold can be pushed outward, past the indefinite folds of index two. To pass each such fold, we require six instances of the C-move, followed by three $R3_3$ moves, followed by six $R2_2$ moves. Then, the above process can be repeated for each indefinite fold of index two, resulting in the simplified diagram shown in Figure 1(c).

Note that the fiber Σ of the central point now has genus $3g$. Choose three rays as in Figure 1(c): The preimages of these rays are genus $3g$ handlebodies, which intersect at their common boundary, Σ. Similarly, the preimages of the regions between the rays are diffeomorphic to $\natural^g(S^1 \times B^3)$. (Each such region is the thickening of a three-dimensional handlebody union $2g$ three-dimensional two-handles that are attached along primitive curves.) Therefore, we have a $(3g, g)$–trisection of X, as desired. □

Note that the base diagram in Figure 1(c) is a simplification of the original base diagram. Baykur and Saeki introduced the notion of a *simple* Morse 2–function, which they defined to be a Morse 2–function whose base diagram consists of disjoint, embedded circles (no cusps) and triangles (three cusps) [5]. They showed that every 4–manifold admits a simplified Morse 2–function, and asked whether every 4–manifold admits a simplified Morse 2–function where the genus of central fiber is minimal for that 4–manifold. The answer to this question seems to be "Yes" for many 4–manifolds [4]. Here, we pose related questions.

Question 3.1. *Does every 4–manifold admit a Morse 2–function whose base diagram consists of a disjoint union of curves, some of which are embedded circles (no cusps) and the rest of which are are immersed with six cusps and three double points, as in Figure 2(e)? If so, does such a Morse 2–function exists where the central fiber is of minimal possible genus for the 4–manifold?*

3.1. From Heegaard diagrams to trisection diagrams

Next, we show how, given a Heegaard diagram for a 3–manifold M, one can produce a trisection diagram for either $\mathcal{S}(M)$ of $\mathcal{S}^*(M)$. Though the distinction between this pair of 4–manifolds was not visible from the Morse 2–function perspective, these manifolds are not, in general, diffeomorphic, so they will necessarily be described by different trisection diagrams.

Theorem 1.4. Let (S, δ, ε) be a genus g Heegaard diagram for a closed 3–manifold M with the property that H_ε is standardly embedded in S^3. Then,

1) the 4–manifold $\mathcal{S}(M)$ admits a trisection diagram that is obtained from (S, δ, ε) via the local modification at each curve of ε shown in Figure 6, and
2) the 4–manifold $\mathcal{S}^*(M)$ admits a trisection diagram that is obtained from (S, δ, ε) via the local modification at each curve of ε shown in Figure 7.

Note that the condition on H_ε is equivalent to the condition that (S, δ, ε) be drawn as in Figure 3.

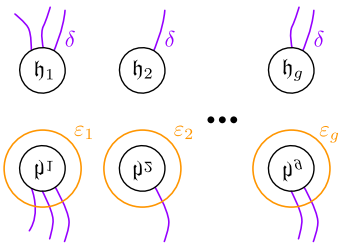

Figure 3: A suitable Heegaard diagram; the ε–curves bound obvious disks in the plane.

Proof. We'll first discuss the the spin $\mathcal{S}(M)$, then modify the argument to address the twisted-spin $\mathcal{S}^*(M)$.

Let $M = H_\delta \cup_S H_\varepsilon$ be a genus g Heegaard splitting for M. We have the following decomposition:

$$\mathcal{S}(M) = (H_\delta \times S^1) \cup_Y (\mathcal{S}(H_\varepsilon)),$$

where $Y = S \times S^1$. This decomposition is visible in Figure 1(b), where Y is the preimage of a circle separating the indefinite folds of index one from

those of index two. In the proof of Theorem 1.2 above, the Morse 2–function was modified on $\mathcal{S}(H_\varepsilon)$ in such a way that the central fiber became a genus $3g$ surface Σ. Our first task is to identify Σ inside $\mathcal{S}(H_\varepsilon)$. Our approach will be to work from Figure 1(b), beginning at the center, and "trisect" each subsequent index two fold.

The space $\mathcal{S}(H_\varepsilon)$ can be obtained from $S^2 \times D^2$ by attaching g round one-handles in the following manner. We will parameterize D^2 by (r, θ) with $r \in [0,1]$ and $\theta \in S^1 \subset \mathbb{C}$, and we will let $\vec{r}_\theta \subset D^2$ denote the unit-length segment at angle θ. For $i = 1, 2, \ldots, g$, let D_i^+ and D_i^- be a pair of disjoint disks on S^2, and attach a three-dimensional one-handle $\mathfrak{h}_i^\theta$ to $S^2 \times \vec{r}_\theta$ along $D_i^\pm \times \{(1,\theta)\}$ for each $\theta \in S^1$. (For each i, the union $\mathfrak{h}_i = \bigcup_\theta \mathfrak{h}_i^\theta$ is a 4–dimensional round one-handle.) Equivalently, we can view this handle attachment as the identification of $D^+ \times \{(1,\theta)\}$ with $D^- \times \{(1,\theta)\}$ via a reflection (conjugation) map. We parameterize $D_i^\pm$ by (s, ϕ), where $s \in [0,1]$ and $\phi \in S^1 \subset \mathbb{C}$, and we let

$$\omega_i^\theta(s,\phi) = ((s,\phi) \times \vec{r}_\theta) \cup (\overline{(s,\phi)} \times \vec{r}_\theta).$$

In other words, the $\omega_i^\theta(s,\phi)$ are arcs that run over $\mathfrak{h}_i^\theta$, connecting identified pairs of points in $D^\pm$ on $S^2 \times \{(0,0)\}$.

Consider the arcs ω_i^θ given by

$$\omega_i^\theta = \omega_i^\theta(1/2,\theta) = ((1/2,\theta) \times \vec{r}_\theta) \cup (\overline{(1/2,\theta)} \times \vec{r}_\theta).$$

In other words, ω_i^θ is an arc running over $\mathfrak{h}_i^\theta$ connecting the point with angle θ on the circle of radius $1/2$ on D_i^+ to the conjugate point on D_i^-. Note that $\mathfrak{h}_i^\theta$ can be regarded as a regular neighborhood of ω_i^θ, so $\mathcal{S}(H_\varepsilon)$ is a regular neighborhood of the two-complex

$$S^2 \cup \left(\bigcup_{i=1}^{g} \bigcup_{\theta \in S^1} \omega_i^\theta \right).$$

Consider the three angle values $\theta_j = \frac{2\pi}{3} j$, for $j = 0, 1, 2$, along with the $3g$ arcs $\omega_i^{\theta_j}$. Let Σ be the surface obtained by surgering the central S^2 along these $3g$ arcs. Note that Σ has genus $3g$ and is contained in the interior of $\mathcal{S}(H_\varepsilon)$. We now describe three compression bodies whose higher genus boundary component coincides with Σ and whose lower genus boundary component is a fiber of $Y = S \times S^1$, hence has genus g. Thus, we must describe $2g$ compression disks for each compression body.

Let $\mathfrak{h}_i^j$ denote a small tubular neighborhood of $\omega_i^{\theta_j}$. We can think of $\mathfrak{h}_i^j$ as a small three-dimensional one-handle inside the larger three-dimensional

one-handle $\mathfrak{h}_i^{\theta_j}$, as in Figure 4. Let $\Delta_{1,i}^j$ denote the cocore of $\mathfrak{h}_i^j$. Next, notice that $\Sigma \cap D_i^+$ is a thrice-punctured disk. These punctures cut the circle of radius $1/2$ in D_i^+ into three arcs. Call these arcs a_i^j, with the value j determined by the property that $a_i^j \cap \mathfrak{h}_i^j = \emptyset$. See Figure 4(a). Let $\Delta_{2,i}^j$ be the union of the arcs ω_i^θ corresponding to the points in arc a_i^j. Note that the $\Delta_{2,i}^j$ are compression disks for Σ.

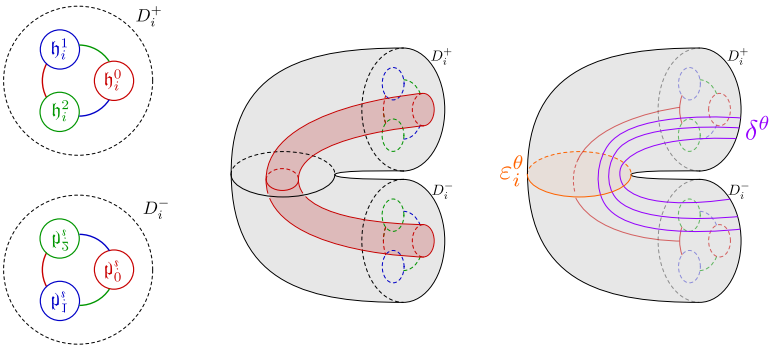

Figure 4: (a) The disk $D_i^\pm$ on the central sphere $S^2 \times \{(0,0)\}$ describing the attaching region for $\mathfrak{h}_i^\theta$. (b) The handle $\mathfrak{h}_i^0$ inside the $\mathfrak{h}_i^{\theta_0}$, and the portion of H_α bounded thereby. (c) The handle $\mathfrak{h}_i^\theta$ for some $\theta \in (2\pi/3, 4\pi/3)$. In the interior, we have the arc ω_i^θ, which lies in the α–disk $\Delta_{2,i}^0$. One the boundary, we have the curve ε_i^θ and potions of the curves from δ, which serve to parameterize the genus g surface $S \times \theta$ in $\partial(\mathcal{S}(H_\varepsilon)) = \partial(H_\delta \times S^1) = S \times S^1$.

Let H^j denote the compression body defined by the disks $\{\Delta_{1,i}^j, \Delta_{2,i}^j\}_{i=1}^g$. Note that Σ is contained in the union

$$S^2 \cup \left(\bigcup_{i=1}^{g} \bigcup_{j=0}^{2} \mathfrak{h}_i^{\theta_j} \right).$$

If we compress Σ using, say, the disks $\Delta_{1,i}^0$, then the resulting surface can be made disjoint from the handles at angle 0. Slightly differently, if we compress further using the disks $\Delta_{2,i}^0$, then Σ can be isotoped to lie in any single angle, say $2\pi/3$. It follows that the result of compressing Σ along the disks $\Delta_{1,i}^0$ and $\Delta_{2,i}^j$ is the surface $S \times \{2\pi/3\}$. Repeating this, we see that the lower genus boundary component of H^j can be assumed to be $S \times \{\theta_j + 2\pi/3\}$, as desired.

Consider the complex $X = \Sigma \cup H^0 \cup H^1 \cup H^2$. This complex is a three-dimensional neighborhood of the two-complex described above. It follows that $\mathcal{S}(H_\varepsilon)$ is obtained by thickening X.

We complete the H^j to handlebodies by attaching a copy of H_δ to the lower genus boundary component. For example, we let $H_\alpha = H^0 \cup (H_\delta \times \{2\pi/3\})$, and we obtain H_β and H_γ from H^1 and H^2 similarly. We claim that $H_\alpha \cup H_\beta \cup H_\gamma$ is the spine of a trisection of $\mathcal{S}(M)$. A regular neighborhood of this spine is given by $\mathcal{S}(H_\varepsilon)$ plus thickening of the three H_δ–fibers. All that remains is to fill in the four dimensional spans between the H_δ–fibers. Each of these pieces is $H_\delta \times I$, which is a 4–dimensional one-handlebody. If follows that this spine defines a $(3g, g)$–trisection of $\mathcal{S}(M)$.

Finally, we will describe a trisection diagram corresponding to this spine by describing the curves α lying on Σ that determine the handlebody H_α. The construction is symmetric in α, β, and γ, so the description of the other curves will follow. Recall that we assumed that the Heegaard diagram (S, δ, ε) was standard, as in Figure 3. Figure 4 shows how to take each handle $\mathfrak{h}_i$ and create from it a triple of handles, $\mathfrak{h}_i^j$, as in the construction of the trisection above. For each i, two α disks are obtained. Let $\alpha_{g+i} = \partial\Delta^0_{1,i}$, and let $\alpha_{2g+i} = \partial\Delta^0_{2,i}$. See Figure 5. Compressing along these $2g$ disks gives the fiber $S \times \{2\pi/3\}$.

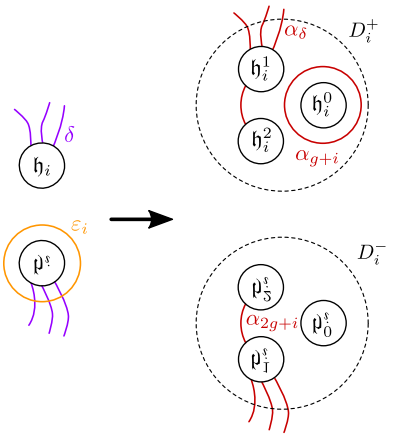

Figure 5: The local transition from a Heegaard diagram (δ, ε) to the α–curves of the trisection diagram (α, β, γ). The β– and γ–curves are obtained in a symmetric way.

Figure 4(c) shows one θ–slice of the round handle $\mathfrak{h}_i$. At each such θ–slice, we see ε_i^θ bounding to the inside, while the curves of δ^θ run over the handle as prescribed by the original diagram (Figure 3). Imagine $\theta = 2\pi/3$

here, and recall that we think of $\mathfrak{h}_i^{2\pi/3}$ as a neighborhood of $\omega_i^{2\pi/3}$ (the arc shown in Figure 4(c)). The disks bounded by the curve δ in $H_\delta \times \{2\pi/3\}$ are almost the remaining α–disks, but their boundary lies on the lower genus boundary component of the compression body H^0, not on Σ. However, it is a simple matter to flow the boundaries of this disk up through the compression body (using the vertical structure) until they lie on Σ.

Thus, for $i = 1, \dots, g$, α_i will be determined by δ_i in the following way. Outside of the $D_i^{\pm}$, α_i coincides with δ_i. Inside, the arcs run from $\partial D_i^{\pm}$ to the handle $\mathfrak{h}_i^1$. In fact, this choice is well-defined, thanks to the presence of the curves α_{g+i} and α_{2g+i}, as in Figure 5. Let $\alpha_\delta = \{\alpha_1, \dots, \alpha_g\}$.

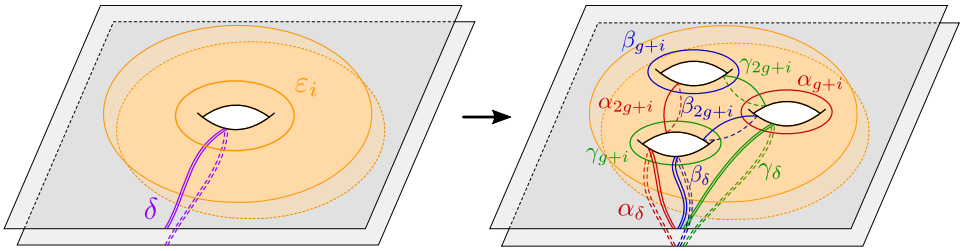

Figure 6: The local modification used to transform a Heegaard diagram (δ, ε) for a 3–manifold M into a trisection diagram (α, β, γ) for the spun manifold $\mathcal{S}^*(M)$.

The sum total of this local modification is shown in Figure 6. Note that the curves α_δ, β_δ, and γ_δ coincide after compressions of the other types of curves. This reflects the fact that these curves come from $H_\delta \times S^1$. This completes the proof of part (1).

To pass from the case of $\mathcal{S}(M)$ to that of $\mathcal{S}^*(M)$, we will perform a Gluck twist on the central S^2, cutting out a $S^2 \times D^2$ neighborhood and re-gluing with a full twist. Importantly, we assume that the twisting takes place in the θ–interval $[0, 2\pi/3]$. Under this assumption, we see that Σ is preserved after the Gluck twist, as are H_α and H_β. Further, the γ_δ and γ_{g+i} are also preserved. The only change occurs to the curves γ_{2g+i}; the Gluck twist is concentrated above the arc a_i^2. The disks γ_{2g+1} sitting above these arcs get twisted around the terminal locus of the arc. In terms of the diagram, this gluing amounts to performing a Dehn twist of the γ_{2g+i} about the corresponding β_{g+i}. Thus, Figure 6 changes to Figure 7. This completes the proof of part (2). □

Note that within the above proof, we have also given a second proof of Theorem 1.2 that is independent of the original Morse 2–function proof.

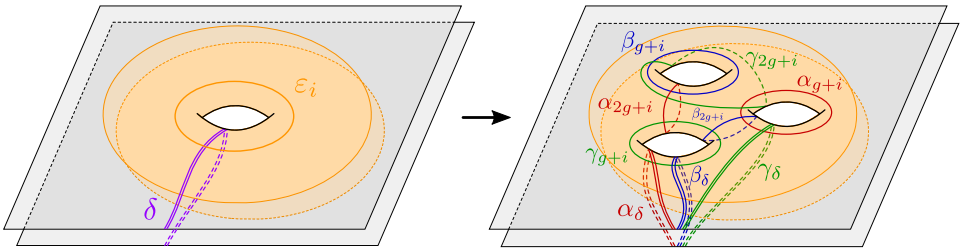

Figure 7: The local modification used to transform a Heegaard diagram (δ, ε) for a 3–manifold M into a trisection diagram (α, β, γ) for the twist-spun manifold $\mathcal{S}^*(M)$.

3.2. Doubly-pointed diagrams

Let M be a closed, connected, orientable 3–manifold, and let K be a knot in M. Let $M = H_1 \cup_S H_2$ be a Heegaard splitting for M. Assume that S has large enough genus (stabilizing if necessary) so that K can be put in 1–bridge position with respect to S. This means that $\upsilon_i = K \cap H_i$ is a properly embedded, boundary-parallel arc for $i = 1, 2$. Let $\{z, w\} = K \cap S$, and assume that υ_1 is contained in the zero-handle $\mathfrak{h}_0$, while υ_2 is contained in the three-handle $\mathfrak{h}_3$.

Theorem 1.5. Let (S, δ, ε) be a genus g Heegaard diagram for a closed 3–manifold M with the property that H_ε is standardly embedded in S^3. Let K be a knot in M such that $(S, \delta, \varepsilon, z, w)$ is a doubly-pointed Heegaard diagram for the pair (M, K). Then the pairs $\mathcal{S}^n(M, K)$ admit doubly-pointed trisection diagrams that are obtained from $(S, \delta, \varepsilon, z, w)$ via a local modification at each curve of ε.

Proof. By the last part of the proof of Theorem 1.4, it is clear that gluing using τ^n corresponds to Dehn twisting γ_{2g+i} n times about β_{g+i}. Thus, the underlying trisection diagram $(\Sigma, \alpha, \beta, \gamma)$ results from the same local modification as in Figure 7, except with the added Dehn twists.

It remains to show that $\mathcal{S}^n(K)$ is in 1–bridge position with respect to this trisection, so we verify that $\mathcal{S}^n(K)$ intersects the three handlebodies in boundary parallel arcs and intersects the 4–dimensional pieces in boundary parallel disks.

The sphere $\mathcal{S}^n(K)$ can be decomposed as

$$D^2 \times \{N\} \cup (\upsilon_1 \times S^1) \cup D^2 \times \{S\}.$$

We now consider how the various parts of this decomposition intersect the trisection of $\mathcal{S}^n(M)$.

Consider $\upsilon_1 \times S^1 \subset H_\delta \times S^1$. This annulus intersects each of fibers in an arc. For example, $\upsilon_1 \times \{2\pi/3\}$ is an arc in $H_\delta \times \{2\pi/3\}$ with endpoints in the lower genus boundary component, $S \times \{2\pi/3\}$, of the compression body H^0. The endpoints of this arc are $\{z, w\} \times \{2\pi/3\}$. Since υ_1 is boundary parallel (in $H_\delta \subset M$) into S, we have that $\upsilon_1 \times \{2\pi/3\}$ is boundary parallel (in $H_\delta \times \{2\pi/3\} \subset H_\alpha$) into $S \times \{2\pi/3\}$ and that the disk $\upsilon_1 \times [0, 2\pi/3]$ is boundary parallel (in $H_\delta \times [0, 2\pi/3]$) into $S \times [0, 2\pi/3]$.

Let us focus now on $\upsilon_\alpha = \mathcal{S}^n(K) \cap H_\alpha$, recalling that

$$H_\alpha = H_\delta \times \{2\pi/3\} \cup_{S\times\{2\pi/3\}} H^0.$$

We have already seen that $\mathcal{S}^n(K) \cap (H_\delta \times \{2\pi/3\}) = \upsilon_1 \times \{2\pi/3\}$ is boundary parallel into $S \times \{2\pi/3\}$. Next, we note that $\mathcal{S}^n(K) \cap H^0$ is simply two arcs. One arc runs from $\{z\} \times \{2\pi/3\}$ to the north pole N of the sphere $S^2 \times \{0\}$ that was the core of the original filling in the twist-spinning operation. Of course, this sphere was stabilized to produce the trisection surface Σ, but these modification were performed away from the poles. Thus, this arc is vertical in the compression body H^0. Similarly, the second arc is vertical and connects $\{w\} \times \{2\pi/3\}$ to the south pole S of Σ. Since Σ and $S \times \{2\pi/3\}$ cobound the compression body H^0 and υ_α is a flat arc in the lower genus side together with two vertical arcs, it follows that υ_α can be isotoped to lie in Σ, as desired. The same goes for the arcs υ_β and υ_γ.

Next, let us focus on the 4–dimensional region X_3 between H_α and H_γ. Recall that $H_\gamma = H^2 \cup H_\delta \times \{0\}$, so we can write

$$X_3 = (H_\delta \times [0, 2\pi/3]) \cup_{S\times[0,2\pi/3]} \left((H^0 \cup_\Sigma H^2) \times I\right).$$

The second piece of the union comes from the fact that $\mathcal{S}^n(H_\varepsilon)$ was seen to be a thickening of the complex $\Sigma \cup H^0 \cup H^1 \cup H^2$. Now, we note that $\mathcal{D}_3 = \mathcal{S}^n(K) \cap X_3$ is simply the disk $\upsilon_1 \times [0, 2\pi/3]$, which we have already observed is boundary parallel into $S \times [0, 2\pi/3]$, together with some vertical pieces in the thickening $(H^0 \cup_\Sigma H^2) \times I$.

Since $\partial\mathcal{D}_3 = \upsilon_\alpha \cup_{\{N,S\}} \upsilon_\gamma$, once we have pushed most of $\mathcal{D}_3$ into $S \times [0, 2\pi/3]$, we can use the product structure of $(H^0 \cup_\Sigma H^2) \times I$ and the boundarly parallelism of υ_α and υ_γ to push $\mathcal{D}_3$ into $H^0 \cup_\Sigma H^2 \subset H_\alpha \cup_\Sigma H_\gamma$, as desired. The same goes for the other 4–dimensional pieces $(X_2, \mathcal{D}_2)$ and $(X_1, \mathcal{D}_1)$.

Thus, $\mathcal{S}^n(K)$ is in 1–bridge position with respect to the trisection described in the proof of Theorem 1.4. Note that the local modification require

here is slightly different: We must twist the γ_{2g+i} around the β_{g+i} a total of n times. However, once we have done that, we have a doubly-pointed diagram for $\mathcal{S}^n(M,K)$; since the double-point $\{z,w\}$ is distant from the ε_i, it is not affected by the modification, and it becomes the double-point $\{N,S\}$ for the doubly-pointed trisection diagram. This completes the proof. (In order to see that $\{N,S\}=\{z,w\}$ in the appropriate manner, we simply treat the original surface S as the boundary of the result of attaching handles to $S^2\times\{0\}$ in the standard way. In other words, if we think of the original double-point $\{z,w\}$ as the "poles" of S, the the new double-point $\{z,w\}=\{N,S\}$ for Σ is simply the "poles" of Σ coming from the poles of $S^1\times\{0\}$.) □

4. Corollaries, examples, and questions

Let us return to the question of classifying manifolds with low trisection genus. The following facts are easy to verify.

1) The only manifold with trisection genus zero is S^4.
2) The only manifolds with trisection genus one are $\mathbb{CP}^2$, $\overline{\mathbb{CP}^2}$, and $S^1\times S^3$.

Moreover, $S^2\times S^2$ is the only irreducible 4–manifold with trisection genus two. We also have the following.

Proposition 4.1. *Suppose X admits a (g,k)–trisection. Then,*

1) $\chi(X)=2+g-3k$.

2) $\pi_1(X)$ has a presentation with k generators.

3) $|H_1(X;\mathbb{Q})|\leq k$ and $|H_2(X;\mathbb{Q})|\leq g-k$.

Proof. Such an X admits a handle decomposition with a single 0–handle, k 1–handles, $g-k$ 2–handles, k 3–handles, and a single 4–handle [13, 27]. □

We can now prove Corollary 1.3. Note that (g,k)–trisections are standard if $k\geq g-1$ [27].

Corollary 1.3. For every integer $g\geq 3$ and every $1\leq k\leq g-2$, there exist infinitely many distinct 4–manifolds admitting minimal (g,k)–trisections.

Proof. Let $l\geq 1$, and let M be a three-manifold with Heegaard genus $g(M)=l$ and $rk(\pi_1(M))=l$. (For example, choose M to be a connected sum of l lens

spaces.) Let $X = \mathcal{S}(M)\#(\#^m\mathbb{CP}^2)$. By Theorem 1.2, and since $\mathbb{CP}^2$ admits a $(1,0)$–trisection, X admits a $(3l+m, l)$–trisection. By Proposition 4.1(2), since $\pi_1(X) = \pi_1(M)$, X cannot admit a (g', k')–trisection with $k' < l$. By Proposition 4.1(1), X cannot admit a (g', l)–trisection with $g' < 3l + m$. In this way, we can produce infinitely many distinct X (distinguished by their fundamental groups) that admit minimal $(3l+m, l)$–trisections for $l \geq 1$ and $m \geq 0$. This proves the corollary in the case that $g \geq 3k$.

Next, let $X' = \mathcal{S}(M)\#(\#^n S^1 \times S^3)$. This time, since $S^1 \times S^3$ admits a $(1,1)$–trisection, X' admits a $(3l+n, l+n)$–trisection. By Grushko's Theorem [18, 33], we have $rk(\pi_1(X')) = l + m$, so this trisection is minimal, as above. Again, infinitely many such X' can be produced and seen to be distinct whenever $l \geq 1$ and $n \geq 0$. This proves the lemma in the case that $g \leq 3k$. □

Conspicuously absent from this result is the case of $k = 0$.

Question 4.2. *For some $g \geq 3$, are there infinitely many 4–manifolds admitting (minimal) $(g,0)$–trisections?*

Since the classification of 4–manifolds with trisection genus three is the first open case, we next turn our attention to the case of spun lens spaces.

4.1. Spinning lens spaces

Figure 8 shows how to obtain a trisection diagram for $\mathcal{S}_5$. The process is general. Start with the genus one Heegaard diagram (δ, ε) for $L(p,q)$ where ε is drawn as the boundary of the disk filling the center hole, and the curve δ is a (p,q)–curve. After performing the local modification, we see the characteristic 6–tuple of curves in the center, encircled by three copies of something similar to a (p,q)–curve. In fact, these three more complicated outer curves will become (p,q)–curves (and will coincide) after the compression of any pair of same colored curve in the center. Let $\mathcal{T}(p,q)$ denote the trisection obtained in this way.

By Corollary 2.4, we know that $\mathcal{S}(L(p,q))$ and $\mathcal{S}^*(L(p,q))$ are diffeomorphic to $\mathcal{S}_p$, independent of q and q'. This raises the following question.

Question 4.3. *Are $\mathcal{T}(p,q)$ and $\mathcal{T}(p,q')$ diffeomorphic as trisections for distinct values of q?*

For completeness, we describe how to obtain diagrams for the $\mathcal{S}'_p$. Although, these diagrams depend on understanding the Gluck twist and surgery

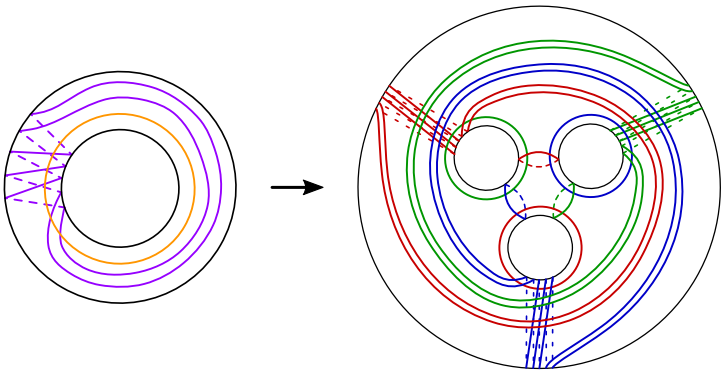

Figure 8: A genus one Heegaard diagram for the lens space $L(5,2)$ is transformed into a genus three trisection diagram for the spun lens space $\mathcal{S}_5 \cong \mathcal{S}(L(5,2))$.

operations from a trisection diagram perspective, the details of which are presented in [16]. The relevant sequence of diagrams is shown in Figure 9. Begin with a diagram for $\mathcal{S}_p$. (In this example, $p = 4$ and the diagram comes from $\mathcal{S}(L(4,1))$.) We place points in the two central hexagons (one on the top of the surface and one on the bottom). Colored arcs are given to show that the points can be connected in the complement of curves of each color. The fact that the arcs can be slid to coincide (paying attention to the relevant color) ensures that this is a doubly-pointed Heegaard triple. Let $\mathcal{K}$ denote the 2–knot in $\mathcal{S}_p$ encoded thusly. We surger the surface along the dots, and extend the colored arcs to curves across the new annulus. The resulting diagram describes the result of surgery on $\mathcal{K}$. An easy exercise shows that this diagram destabilizes to give the genus one diagram for $S^1 \times S^3$. (This proves that we identified the correct 2–knot.) Finally, the third diagram describes the result of performing a Gluck twist on $\mathcal{K}$ in $\mathcal{S}_p$, which, by definition, gives $\mathcal{S}'_p$. Details justifying these diagrammatic changes appear in [16]. The interested reader should compare Figure 9 with recent work of Dale Koenig [26], where trisections of 3–manifold bundles over S^1 are studied.

Remark 4.4. The right diagram in Figure 9 is obtained from the left one by a Dehn twist of one γ–curve about a β–curve. If we had twisted the other γ–curve about the other β–curve, we would have a diagram for $\mathcal{S}^*(L(p,q))$, as described by Theorem 1.4.

Baykur and Saeki have independently identified the manifolds in $\mathcal{P}$ as admitting simplified genus three trisections [4, 5]. The proof of Theorem 1.2

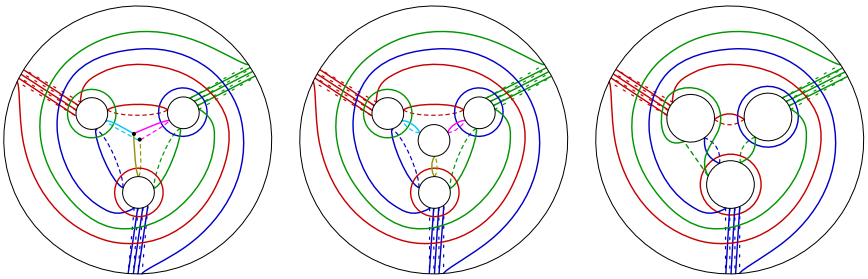

Figure 9: (Left) A doubly-pointed trisection diagram encoding the relevant 2–knot in $\mathcal{S}_p$. (Middle) The trisection diagram corresponding to the result of performing surgery on this 2–knot in $\mathcal{S}_p$. An easy exercise shows that this diagram destabilizes to give the standard diagram for $S^1 \times S^3$. (Right) The diagram corresponding to the result of performing a Gluck twist on this 2–knot in $\mathcal{S}_p$; i.e., the sibling manifold $\mathcal{S}'_p$. (Here, $p = 4$.)

gives a different type of "simplified" trisection for these spaces. (See Question 3.1 above.) This leads to the the following questions.

Questions 4.5.

1) *If X admits a simplified genus three trisection (in either sense), is $X \in \mathcal{P}$?*

2) *If X admits a genus three trisection, does X admit a simplified genus three trisection?*

4.2. Spinning homology spheres

Let $\Sigma(p, q, r)$ denote the homology sphere that is a Seifert fibered space over the base orbifold $S^2(p, q, r)$. Such spaces are known as *Brieskhorn spheres*. When $pq + qr + rp = \pm 1$, we can consider $\Sigma(p, q, r)$ as the branched double cover of S^3 along the pretzel knot $P(p, q, r)$. In this case, it is particularly easy to give a genus two Heegaard splitting for $\Sigma(p, q, r)$ via the 3–bridge splitting of $P(p, q, r)$. Such a diagram is shown on the left in Figure 10 in the case of $\Sigma(-2, 3, 5)$, which is the Poincaré homology sphere.

Figure 10 shows how to obtain a trisection diagram for $\mathcal{S}(\Sigma(p, q, r))$ when $pq + qr + rp = \pm 1$. As far as we know, these are the simplest possible trisection diagrams for homology 4–spheres.

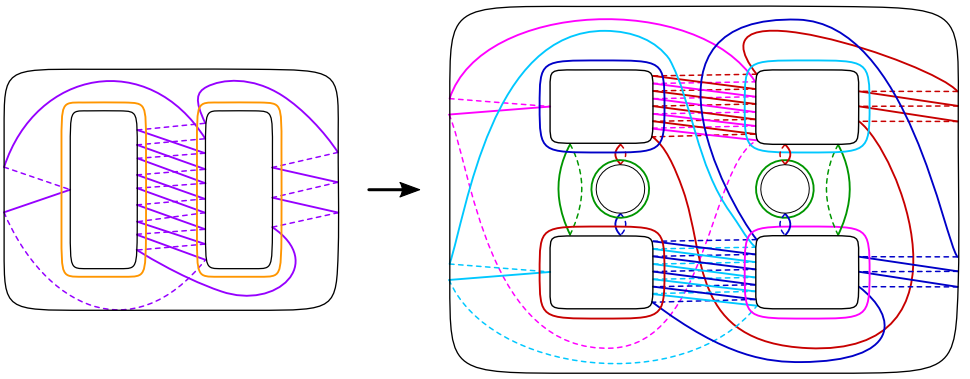

Figure 10: (Left) A Heegaard splitting for the Poincaré homology sphere $\Sigma(-2,3,5)$. (Right) A trisection diagram for $\mathcal{S}(\Sigma(-2,3,5))$. Note that two of the γ–curves (green) are not shown, but can be taken to be the same as the two complicated α–curves (red/pink).

4.3. Spinning a Boileau-Zieschang space

In 1984, Boileau and Zieschang exhibited a family of Seifert fibered spaces whose members have Heegaard genus three but fundamental groups of rank two [7], showing that these two complexity measures of a three-manifold do not always coincide. Proposition 4.1 states that if X admits a (g,k)–trisection, then $rk(\pi_1(X)) < k$, so we pose the following, analogous question in dimension four.

Question 4.6. *Does there exist a 4–manifold X such that every (g,k)–trisection of X satisfies $k > rk(\pi_1(X))$?*

The answer to this question is almost certainly affirmative; however, there are presently no tools capable of bounding the value of k away from $rk(\pi_1(X))$. A logical first step towards the resolution of this question would be to consider the spins of the Boileau-Zieschang manifolds, the simplest of which is the Seifert fibered space $Y = S^2(-1/2,-1/2,1/2,-1/3)$ and can be described as the double cover of S^3 branched along the pretzel knot $P(-2,-2,2,-3)$. Figure 11 gives a genus three (minimal) Heegaard diagram for Y and the corresponding $(9,3)$–trisection diagram for the spin $\mathcal{S}(Y)$, which may or may not be minimal. We pose the following question with this example in mind.

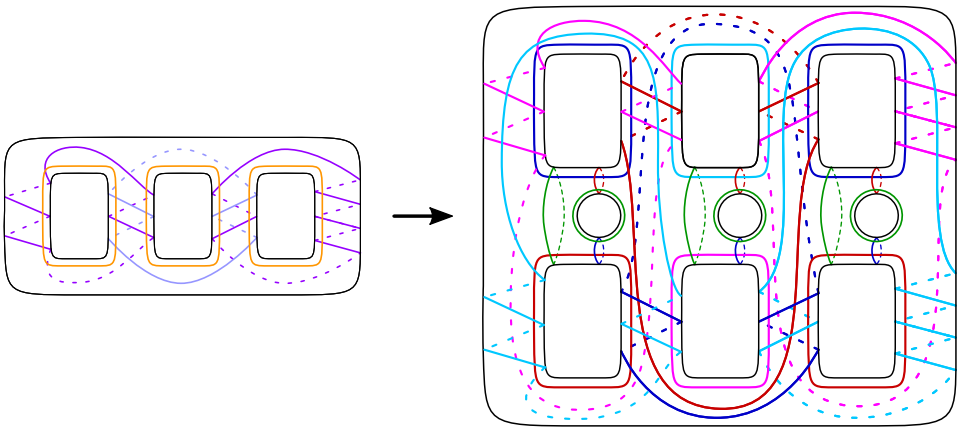

Figure 11: (Left) A Heegaard splitting for the Boileau-Zieschang Seifert fibered space $Y = S^2(1/2, -1/2, 1/2, -1/3)$. (Right) A trisection diagram for its spin $\mathcal{S}(Y)$. Note that three of the γ–curves (green) are not shown, but can be taken to be the same as the three complicated α–curves (red/pink).

Questions 4.7. *If $\mathcal{H}$ is a irreducible Heegaard splitting, is $\mathcal{S}(\mathcal{H})$ (as constructed above) necessarily irreducible?*

Note that it is an easy consequence of the construction above and Haken's Lemma [20] that $\mathcal{S}(\mathcal{H})$ will be reducible whenever $\mathcal{H}$ is.

4.4. Spinning manifold pairs

We conclude by presenting two diagrams of spun pairs, one coming from a knot in S^3 and the other coming from a knot in a lens space. First, consider the doubly-pointed diagram for the torus knot $T(3,4)$ shown on the left in Figure 12. One interesting property about torus knots is that the bridge number of $T(p,q)$ is equal to $\min(p,q)$. This was used in [29] to show that the spins $\mathcal{S}(T(p,q))$ have bridge number $3\min(p,q)+1$. On the other hand, every torus knot can be isotoped to lie on the genus one Heegaard splitting of S^3, and, therefore, $T(p,q)$ admits a doubly-pointed genus one Heegaard diagram. It follows, as is shown on the right side of Figure 12, that $\mathcal{S}(T(p,q))$ admits a doubly-pointed genus three trisection diagram.

Next, let $Y = L(7,3)$, and let K be the knot described by the doubly-pointed Heegaard diagram on the left side of Figure 13. The knot K is an example of a knot in Y that has a surgery to S^3. (See [22] for an overview

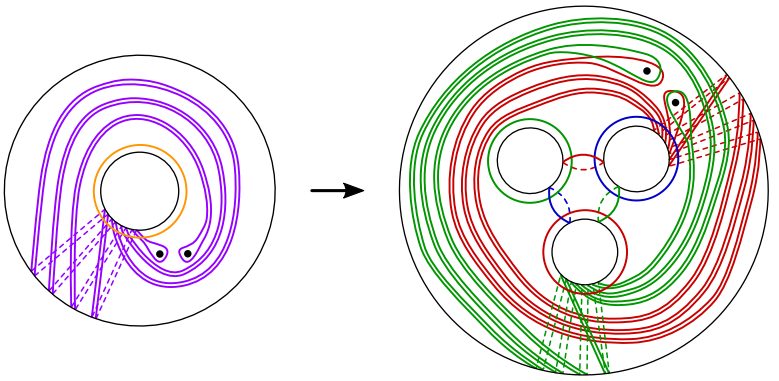

Figure 12: (Left) A doubly-pointed Heegaard splitting for the torus knot $T = T(3,4)$. (Right) A doubly-pointed trisection diagram for the pair $\mathcal{S}(S^3, T)$. Note that the third β–curve (blue) is not shown, but can be assumed to coincide with the complicated γ-curve (green).

of these so-called *simple knots*.) Figure 13 shows the corresponding doubly-pointed trisection diagram for $\mathcal{S}(Y, K)$.

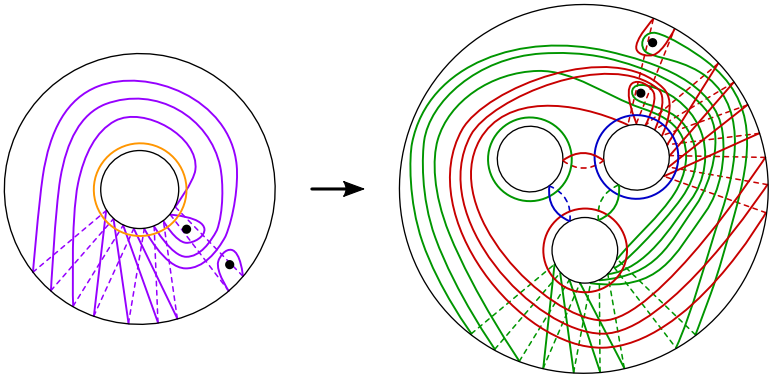

Figure 13: (Left) A doubly-pointed Heegaard splitting for a simple knot K in $L(7,3)$. (Right) A doubly-pointed trisection diagram for the pair $\mathcal{S}(L(7,3), K)$. Note that the third β–curve (blue) is not shown, but can be assumed to coincide with the complicated γ-curve (green).

Acknowledgements

This article was inspired by conversations with Alex Zupan, who gave a preliminary sketch of the proof of Theorem 1.2. The author is also grateful to R.

İnanç Baykur for helpful conversations that gave a singularity theory context to the present work and for comments that improved the exposition of the article throughout. The author would like to thank the anonymous referee for carefully reading the article and making a number of useful comments. This work was supported by NSF grants DMS-1400543 and DMS-1758087.

References

[1] Aaron Abrams, David T. Gay, and Robion Kirby, *Group trisections and smooth* 4*-manifolds*, Geom. Topol. **22** (2018), no. 3, 1537–1545.

[2] E. Artin, *Zur Isotopie zweidimensionaler Flächen im* R_4, Abh. Math. Sem. Univ. Hamburg **4** (1925), no. 1, 174–177.

[3] R. I. Baykur and S. Kamada, *Classification of broken Lefschetz fibrations with small fiber genera*, J. Math. Soc. Japan **67** (2015), no. 3, 877–901.

[4] R. İnanç Baykur and Osamu Saeki, *Simplified broken lefschetz fibrations and trisections of* 4*-manifolds*, Proceedings of the National Academy of Sciences **115** (2018), no. 43, 10894–10900.

[5] R. I. Baykur and O. Saeki, *Simplifying indefinite fibrations on* 4*–manifolds*, `arXiv:1705.11169`, (2017).

[6] R. H. Bing, *An alternative proof that* 3*-manifolds can be triangulated*, Ann. of Math. (2) **69** (1959), 37–65.

[7] M. Boileau and H. Zieschang, *Heegaard genus of closed orientable Seifert* 3*-manifolds*, Invent. Math. **76** (1984), no. 3, 455–468.

[8] N. A. Castro, *Relative trisections of smooth* 4*–manifolds with boundary*, Ph.D. thesis, University of Georgia (2016).

[9] N. A. Castro, *Trisecting smooth* 4*–dimensional cobordisms*, `arXiv:1703.05846`, (2017).

[10] Nickolas A. Castro, David T. Gay, and Juanita Pinzón-Caicedo, *Diagrams for relative trisections*, Pacific J. Math. **294** (2018), no. 2, 275–305.

[11] Nickolas A. Castro, David T. Gay, and Juanita Pinzón-Caicedo, *Trisections of* 4*-manifolds with boundary*, Proceedings of the National Academy of Sciences **115** (2018), no. 43, 10861–10868.

[12] N. A. Castro and B. Ozbagci, *Trisections of* 4*–manifolds via Lefschetz fibrations*, arXiv:1705.09854, (2017).

[13] D. Gay and R. Kirby, *Trisecting* 4*-manifolds*, Geom. Topol. **20** (2016), no. 6, 3097–3132.

[14] D. T. Gay, *Trisections of Lefschetz pencils*, Algebr. Geom. Topol. **16** (2016), no. 6, 3523–3531.

[15] D. T. Gay, *Functions on surfaces and constructions of manifolds in dimensions three, four and five*, arXiv:1701.01711, (2017).

[16] David Gay and Jeffrey Meier, *Doubly pointed trisection diagrams and surgery on 2-knots*, arXiv:1806.05351, (2018).

[17] H. Gluck, *The embedding of two-spheres in the four-sphere*, Trans. Amer. Math. Soc. **104** (1962), 308–333.

[18] I. Gruschko, *Über die Basen eines freien Produktes von Gruppen*, Rec. Math. [Mat. Sbornik] N.S. **8 (50)** (1940), 169–182.

[19] Sergei Gukov, *Trisecting non-Lagrangian theories*, J. High Energy Phys. (2017), no. 11, 178, front matter + 49.

[20] W. Haken, *Some results on surfaces in* 3*-manifolds*, in: Studies in Modern Topology, 39–98, Math. Assoc. Amer. (distributed by Prentice-Hall, Englewood Cliffs, N.J.) (1968).

[21] K. Hayano, *On genus-*1 *simplified broken Lefschetz fibrations*, Algebr. Geom. Topol. **11** (2011), no. 3, 1267–1322.

[22] M. Hedden, *On Floer homology and the Berge conjecture on knots admitting lens space surgeries*, Trans. Amer. Math. Soc. **363** (2011), no. 2, 949–968.

[23] Gabriel Islambouli, *Comparing* 4*-manifolds in the pants complex via trisections*, Algebr. Geom. Topol. **18** (2018), no. 3, 1799–1822.

[24] K. Johannson, Topology and Combinatorics of 3-Manifolds, Vol. 1599 of Lecture Notes in Mathematics, Springer-Verlag, Berlin (1995). ISBN 3-540-59063-3.

[25] Michael Klug, *Functoriality of group trisections*, Proceedings of the National Academy of Sciences **115** (2018), no. 43, 10875–10879.

[26] D. Koenig, *Trisections of* 3*–manfiold bundles over* S^1, arXiv:1710.04345, (2017).

[27] J. Meier, T. Schirmer, and A. Zupan, *Classification of trisections and the Generalized Property R Conjecture*, Proc. Amer. Math. Soc. **144** (2016), no. 11, 4983–4997.

[28] J. Meier and A. Zupan, *Genus-two trisections are standard*, Geom. Topol. **21** (2017), no. 3, 1583–1630.

[29] J. Meier and A. Zupan, *Bridge trisections of knotted surfaces in* S^4, Trans. Amer. Math. Soc. **369** (2017), no. 10, 7343–7386.

[30] J. Meier and A. Zupan, *Bridge trisections of knotted surfaces in* 4*-manifolds*, Proceedings of the National Academy of Sciences **115** (2018), no. 43, 10880–10886.

[31] J. Meier and A. Zupan, *Characterizing dehn surgeries on links via trisections*, Proceedings of the National Academy of Sciences **115** (2018), no. 43, 10887–10893.

[32] E. E. Moise, *Affine structures in* 3*-manifolds. V. The triangulation theorem and Hauptvermutung*, Ann. of Math. (2) **56** (1952), 96–114.

[33] B. H. Neumann, *On the number of generators of a free product*, J. London Math. Soc. **18** (1943), 12–20.

[34] P. S. Pao, *The topological structure of* 4*-manifolds with effective torus actions. I*, Trans. Amer. Math. Soc. **227** (1977), 279–317.

[35] S. P. Plotnick, *Equivariant intersection forms, knots in* S^4*, and rotations in* 2*-spheres*, Trans. Amer. Math. Soc. **296** (1986), no. 2, 543–575.

[36] K. Reidemeister, *Zur dreidimensionalen Topologie*, Abh. Math. Sem. Univ. Hamburg **9** (1933), no. 1, 189–194.

[37] J. H. Rubinstein and S. Tillmann, *Multisections of piecewise linear manifolds*, `arXiv:1602.03279`, (2016).

[38] Adam Saltz, *Invariants of knotted surfaces from link homology and bridge trisections*, `arXiv:1809.06327`, (2018).

[39] J. Singer, *Three-dimensional manifolds and their Heegaard diagrams*, Trans. Amer. Math. Soc. **35** (1933), no. 1, 88–111.

[40] A. I. Suciu, *The oriented homotopy type of spun* 3*-manifolds*, Pacific J. Math. **131** (1988), no. 2, 393–399.

[41] E. C. Zeeman, *Twisting spun knots*, Trans. Amer. Math. Soc. **115** (1965), 471–495.

Department of Mathematics, University of Georgia
Athens, GA 30602, USA
E-mail address: jeffrey.meier@uga.edu

Received September 18, 2017